IEEE Access
Multidisciplinary | Rapid Review | Open Access Journal

Received February 6, 2017, accepted March 7, 2017, date of publication March 10, 2017, date of current version April 24, 2017.

Digital Object Identifier 10.1109/ACCESS.2017.2681124

Novel Node Deployment Strategies in Corona Structure for Wireless Sensor Networks

WEI KUANG LAI[1], (Senior Member, IEEE), AND CHUNG-SHUO FAN[2]
[1]Department of Computer Science and Engineering, National Sun Yat-sen University, Kaohsiung 804, Taiwan
[2]Department of Information Management, Hsuan Chuang University, Hsinchu 300, Taiwan

Corresponding author: C.-S. Fan (csfan@hcu.edu.tw)

ABSTRACT Owing to the traffic pattern of wireless sensor networks (WSNs), cluster heads (CHs) around the sink node have larger relaying loads and consume their energy more quickly. This paper first analyzes the corona model. Based on analysis results, we find that nearly balanced energy consumption of WSNs can be achieved with the additional help of arranging different initial conditions. We then propose the energy-balanced node deployment with a balanced energy (END-BE) algorithm and END with a maximum lifetime (END-MLT) scheme, which determine the cluster density for each corona according to the energy consumption of each CH. Simulation results show that the energy consumption is nearly balanced by implementing END-BE, and the network lifetime is greatly improved by adopting END-MLT.

INDEX TERMS Clustering methods, energy conservation, wireless sensor networks.

I. INTRODUCTION

Thanks to the rapid development of wireless communications and integrated circuits, micro-electro mechanical systems (MEMS) technologies have improved drastically in terms of cost, size, and sensitivity. A traditional wireless sensor network (WSN) is formed by a sink node and a large number of sensor nodes. Basically, each sensor node is equipped with the capabilities of sensing, computation, and communication. These sensor nodes can be deployed to monitor the sensing field. After sensor nodes are deployed, WSNs require no human intervention in most cases. Moreover, sensor nodes are usually limited by batteries that cannot be recharged. Therefore, energy efficiency becomes a critical problem and a challenge in designing WSNs. Applications of WSN technology includes underground applications [1], environmental monitoring [2], [3], military field surveillance [4], and home automation [5].

It is well recognized that many clustering algorithms can reduce energy consumption, improve scalability, and prolong network lifetime (it is defined as the elapsing time until the first sensor node uses up its energy). In a typical cluster-based WSN, sensor nodes are organized into clusters. These clusters elect a cluster head (CH) node within a cluster. The CH is responsible for collecting the sensed data from cluster members, aggregating data, and transmitting data to the sink node via a multihop path through intermediate CHs. Thus, the use of cluster techniques not only shortens the transmission distances for sensor nodes but also reduces energy consumption; however, each cluster imposes a larger load on the CH. Under this situation, CHs closer to the sink tend to use up their batteries faster than those farther away from the sink due to unbalanced traffics among CHs. To overcome the problem of unbalanced traffics, we focus on novel node deployment methods to balance energy consumption among sensor nodes. We first prove that the balanced energy consumption can achieve maximum throughput (in Theorem 4.1). Then, we prove that balanced energy consumption can achieve maximum network lifetime (in Theorem 4.2). In addition, we find that balanced energy consumption is shown to be impossible if both the cluster radius of each corona and initial energy of each sensor node are the same (in Theorem 4.3). Finally, we show that nearly balanced energy consumption among sensor nodes is shown to be reachable when certain conditions are met (in Theorem 4.4). Therefore, we propose the energy-balanced node deployment with balanced energy (END-BE) algorithm and the energy-balanced node deployment with maximum life-time (END-MLT) algorithm to calculate how many sensor nodes should be deployed in each corona while achieving different objectives. The main contributions of this paper are summarized as follows:

1) The cluster density of each corona is suggested according to the energy consumption of each CH.

To alleviate the load imposed on the CH around the sink, END-BE and END-MLT schemes calculate the density for

each corona. To the best of our knowledge, none of the existing papers provide explicit numerical calculations for the cluster density of each corona. We expect the residual energy of each CH to be almost the same due to the adoption of END-BE, so that CHs near the BS do not drain their batteries more quickly. In addition, END-MLT can further extend the network lifetime by arranging appropriate sensor nodes (with initial energy $\varepsilon_k = 1$) in the outermost corona.

2) Balanced energy consumption of the whole network is shown to be impossible if both the cluster radius of each corona and initial energy of each sensor node is the same.

We show that the balanced energy consumption is impossible if both the cluster radius of each corona and initial energy (ε_i) of each sensor node are the same. This circumstance is due to the many-to-one communication pattern in WSNs.

3) Nearly balanced energy consumption among sensor nodes is shown to be reachable when certain conditions are met.

Under different initial conditions, we demonstrate that nearly balanced energy consumption of the whole network is possible when $0 < \frac{\varepsilon_k}{\varepsilon_{k-1}} < 1$ and $0 < \frac{\rho_{i-1} \times a_{i-1}}{\rho_i \times a_i + \rho_{i-1} \times a_{i-1}} < 1$ (as shown in Section IV.B), where ρ_i is the node density in corona C_i, and a_i is the number of clusters in corona C_i. This important finding also provides the guideline for deploying sensor nodes in corona-based WSNs.

The rest of this paper is organized as follows: Section II surveys related works. Section III discusses the assumptions, network model, and definitions to be used later. Section IV analyzes the various factors for the nonuniform corona model. According to the analysis results, two novel node deployment strategies are proposed in detail in Section V. Section VI discusses the simulation results. Finally, Section VII concludes the paper.

II. RELATED WORK

In the past, mathematical analysis of the coverage and network lifetime has focused on uniformly distributed WSNs. Li and Mohapatra [6] proposed a mathematical model to deal with the energy hole problem [7] in a corona-based WSN. The authors also investigated several possible approaches to mitigate this problem. Olariu and Stojmenovic [8] analyzed how to avoid the energy hole problem under uniformly deployed WSNs with periodic data collection. According to their observations, the energy consumed is minimized if the transmission range of each sensor node is properly adjusted in the equal-width corona-based WSN; however, it may result in unbalanced energy consumption.

Many deployment schemes have attempted to fully cover a sensing field through the use of minimum sensor nodes. Chang *et al.* [9] proposed an efficient obstacle-resistant robot deployment algorithm to achieve full coverage in the sensing field. Halder and Ghosal [10] investigated a coverage problem related to visual sensor networks. Rout and Roy [11] proposed a localized self-deployment scheme for the deployment of randomly scattered sensor nodes to cover predefined targets while maintaining connectivity with the base station (BS) in the presence of obstacles.

Deploying additional relay nodes around the sink also can solve the energy unbalance problems. Ergen and Varaiya [12] assumed that the locations of the relay nodes are predetermined. They formulated the problem as a nonlinear programming problem and then proposed a heuristic approach to solve this problem by restricting the locations of relay nodes within a square cell. Howitt and Wang [13] tried to balance between the energy consumption problem and the segmentation of space. According to analysis results, their proposed energy balanced chain (EBC) scheme performs significantly better than typical hop-by-hop transmissions. Ababnah and Natarajan [14] proposed a novel optimal control theory-based formulation of the sensor deployment problem. Because the complexity of the optimal control-based method is high, the authors designed a low-complexity approximation called the max deficiency algorithm. Simulation results showed that the proposed method requires 10% to 30% fewer sensor nodes than existing approaches.

There had been extensive research on nonuniform sensor distribution strategies in WSN. Lian *et al.* [15] attempted to increase the total data capacity by considering the energy consumed in the data transmissions. The authors observed that static models with uniformly distributed sensor nodes are unable to effectively utilize their energy; that is, after the network lifetime terminates, there is still a large amount of residual energy unused, which can be up to 90% of total initial energy. Liu *et al.* [16] presented a nonuniform distribution strategy according to a general sensor application model. They derived a distribution function to determine the number of sensor nodes associated with the distance to the sink. They also assumed that each sensor is required to report the sensed data to the sink periodically. Simulation results show that the proposed scheme can prolong the network lifetime. Olariu and Stojmenovic [17] attempted to avoid the energy hole problem by adopting a nonuniform node distribution strategy. Considering the energy consumption for data transmissions, the authors claimed that balanced energy consumption can be obtained when the node density ρ_i in corona i is proportional to $(k + 1 - i)$, where k is the number of coronas. In this case, sensor nodes closer to the sink have to send data with lower rates.

Wu *et al.* [18] proposed a novel node distribution strategy, which is compared to our two proposed schemes in later simulations. They addressed the theoretical aspects of the nonuniform node distribution strategy to mitigate the energy hole problem. It consists of the node distribution strategy and the q-switch routing.

The node distribution strategy: They assumed that sensor nodes are deployed beforehand from the outermost corona C_k to the innermost corona C_1, thus satisfying the constraint:

$$\frac{N_i}{N_{i+1}} = \begin{cases} q, & 1 \le i \le K-2 \\ q-1, & i = K-1, \end{cases} \tag{1}$$

where N_i denotes the number of sensor nodes in corona C_i. That is, the number of sensor nodes have geometric proportion with a ratio $q(>1)$ from corona C_{k-1} to corona C_1. For example, for $q = 3$, $K = 4$, and $N_4 = 8$, it deploys $8 \times 2 = 16$, $16 \times 3 = 48$, and $48 \times 3 = 144$ sensor nodes into corona C_3, C_2, and C_1, respectively.

The q-switch routing in WSNs: The q-switch routing is the shortest path-routing algorithm based on the residual energy. They call it "'q-switch routing'' [18] because each sensor node has q (or $q-1$) relay candidates in the adjacent inner corona. Each sensor node selects one relay node with maximum residual energy for the purpose of distributing energy consumption evenly among relay nodes. The sensor node can switch to the next relay candidate successively because only one node among the q (or $q-1$) relay candidates is selected to forward data in each round. This selection process is repeated until the data are sent to a sensor node in the innermost corona C_1. Then, the data can be delivered to the sink.

According to simulation results, the energy hole problem can be mitigated. Wu *et al*. also proved that their scheme can achieve the sub-balanced energy consumption, which is well-balanced among coronas C_1 to C_{k-1}, except for the outermost corona C_k.

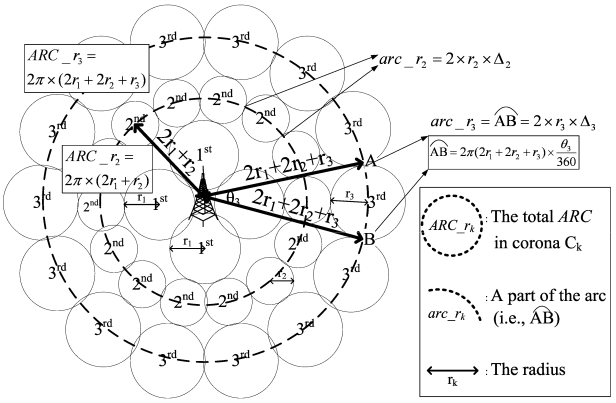

FIGURE 1. Example of three-corona model.

III. PRELIMINARIES

A. ASSUMPTIONS AND NETWORK MODELS

In this paper, we assume that all sensor nodes are deployed in a circular area with a radius of R. The static sink with unlimited energy is located at the center of the topology. Assume that sensor nodes can recognize their geographical position and the position of the sink via exchanging information. A corona model is further considered by dividing the circular area into several coronas. The i th corona is denoted as C_i with each corona having the same width. The C_i is divided into several clusters $CS_{i,j}$ with the same cluster radius (r_i), where i denotes the i th corona, and j represents the order of the cluster in that corona (as illustrated in Fig. 1 with three levels of coronas).

Given that the total radius of topology (R), the number of coronas (K), and $r_i = r_j$, $\forall i, j \neq 0$ and $r_0 = 0$. Assume that the maximum number of coronas ($max\ K$) is 6. Let a_i denote the number of clusters in corona C_i (let $a_1 = 4$), then a_i can be obtained approximately:

$$a_i \approx \frac{\pi \times (\sum_{n=1}^{i} 2r_n)^2 - \pi \times (\sum_{n=1}^{i-1} 2r_n)^2}{\pi \times (r_i)^2}, \quad \forall i = 2 \ldots 6. \tag{2}$$

TABLE 1. The number of clusters after logical partition in each corona

Logical partition in each corona	a_1	a_2	a_3	a_4	a_5	a_6
Original clusters	4	12	20	28	36	44
New clusters	4	12	24	48	48	48

In addition, the logical partition of clusters in each corona is further considered for the purpose of load balancing between clusters of adjacent coronas. From Table 1, we see that a_1 and a_2 remain unchanged because the ratio of a_1 to a_2 is an integer; that is, the relaying capacity delivered from CHs in corona C_2 is equally shared by CHs in corona C_1 (as mentioned later in Section V.C). The ratio of a_{i-1} to a_i (in original clusters), however, is not an integer, $\forall i = 3 \cdots 6$. For this reason, an adjustment is done to even out the shares of each cluster. Specifically, we let the number of original clusters between 28 and 44 be 48. After logical partition is implemented, the ratio of a_{i-1} to a_i is an integer, $\forall i = 2 \cdots 6$.

We assume that each sensor node generates and transmits 1 bit of data per unit time to the sink via multihop communications. We use the energy depletion model proposed in [19]. The energy consumption for transmitting l data unit over a distance of d is $l \times (E_{elec} + E_{amp} \times d^{\alpha})$, where E_{elec} is the energy used in a sensor node for transmitting 1 bit of data, E_{amp} is the amplifier energy (multipath model), d refers to the maximum transmission range, and α indicates the path loss exponent.

B. DEFINITIONS

Definition 3.1: Let ε_{i_m} and $\sum_{rd=1}^{T} E_m^r$, respectively, denote the initial energy of sensor node m in corona C_i and the energy consumption of the sensor node m after round T. The residual energy (RE_m^T) of the sensor node m after round T is defined as

$\varepsilon_{i_m} - \sum_{rd=1}^{T} E_m^r$, where $1 \leq m \leq N$, and N is total number of sensor nodes.

The definition of a round is that one packet is transferred from the sensor node via the CH to the sink. According to the energy conservation law, residual energy of the sensor node m is equivalent to the initial energy of sensor node m minus energy consumption. Therefore, $RE_m^T = \varepsilon_{s_m} - \sum_{rd=1}^{T} E_m^r$.

Definition 3.2: The lifetime (LT_m) of the sensor node m is defined as the maximum number of rounds before the sensor node m depletes its energy: $\max_{T}(\varepsilon_{i_m} \geq \sum_{r=1}^{T} E_m^r)$.

The lifetime of the sensor node m (LT_m) can be interpreted as follows: suppose after T rounds, the residual energy (RE_m^T) is still ≥ 0; but after T +1 rounds, RE_m^T becomes < 0. Then the lifetime of the sensor node m (LT_m) is T rounds.

Definition 3.3: The lifetime (LT) of a sensor network is defined as the minimum number of rounds before any sensor node k depletes its energy: $\min_{k}(LT_k)$

Definition 3.4: Balanced energy consumption is achievable only if

$$\frac{N_1 \times \varepsilon_1}{E_1} = \frac{N_2 \times \varepsilon_2}{E_2} = \cdots = \frac{N_{i-1} \times \varepsilon_{i-1}}{E_{i-1}} = \frac{N_i \times \varepsilon_i}{E_i}, \quad \forall i = 1 \cdots K,$$

where N_i is the number of cluster member in cluster $CS_{i,j}$, ε_i is the initial energy of each sensor node in corona C_i and E_i is the total energy consumption of each CH in corona C_i.

IV. ANALYSIS OF THE CORONA MODEL

In this section, we derive several results for the corona model. First, energy consumption analyses for different coronas are given. Second, we show that balanced energy consumption is not achievable when $r_i = r_j$ and $\varepsilon_i = \varepsilon_j$, $\forall i, j \neq 0$, $i \neq j$. Last, but not least, we demonstrate that nearly balanced energy consumption of the whole network is possible when $0 < \frac{\varepsilon_k}{\varepsilon_{k-1}} < 1$ and $0 < \frac{\rho_{i-1} \times a_{i-1}}{\rho_i \times a_i + \rho_{i-1} \times a_{i-1}} < 1$, where ρ_i is the node density in corona C_i, and a_i is the number of clusters in corona C_i as previously mentioned.

A. ENERGY CONSUMPTION ANALYSIS

Let r_i and ρ_i denote the cluster radius and the node density in corona C_i, respectively. Let N_i denote the number of sensor nodes in a cluster $CS_{i,j}$, that is,

$$N_i = \pi \times (r_i)^2 \times \rho_i. \tag{3}$$

Assume that each sensor node transmits 1 bit of data to its CH. The transmission range is measured between the centers of two clusters for the sake of simplicity in calculations. Let DA_i denote the data aggregation ratio in corona C_i. Basically, each CH in outermost corona C_k only processes the data transmitted by its own cluster members. Because its transmission range is $(r_k + r_{k-1})$, the total energy consumption of a CH in the outermost corona C_k is $N_k \times DA_k \times [E_{elec} + E_{amp} \times (r_k + r_{k-1})^{\alpha}]$. Note that $\alpha = 4$ is often used and is used in the following sections. But α is not limited to 4 for our proposed scheme.

However, each CH in corona C_{k-1} not only processes data given by their cluster members, but it also takes care of data relaying for corona C_k. Because its transmission range is $(r_{k-1} + r_{k-2})$, the total energy consumption of a CH in corona C_{k-1} is

$$[N_{k-1} \times DA_{k-1} + N_k \times DA_k \times \frac{a_k}{a_{k-1}}] \times [E_{elec} + E_{amp} \times (r_{k-1} + r_{k-2})^4].$$

In this way, the total energy consumption of a CH in each corona is

$$\begin{aligned}
E_k &= N_k \times DA_k \times [E_{elec} + E_{amp} \times (r_k + r_{k-1})^4] \\
E_{k-1} &= [N_{k-1} \times DA_{k-1} + N_k \times DA_k \times \frac{a_k}{a_{k-1}}] \\
&\quad \times [E_{elec} + E_{amp} \times (r_{k-1} + r_{k-2})^4] \\
E_{k-2} &= [N_{k-2} \times DA_{k-2} + N_{k-1} \times DA_{k-1} \times \frac{a_{k-1}}{a_{k-2}} \\
&\quad + N_k \times DA_k \times \frac{a_k}{a_{k-2}}] \\
&\quad \times [E_{elec} + E_{amp} \times (r_{k-2} + r_{k-3})^4] \\
&\vdots \\
E_1 &= [N_1 + \sum_{i=2}^{k} N_i \times \frac{a_i}{a_1}] \times [E_{elec} + E_{amp} \times (r_1)^4]
\end{aligned} \tag{4}$$

B. BALANCED ENERGY CONSUMPTION

Theorem 4.1: Balancing the energy consumption among sensor nodes can achieve maximum throughput.

Proof: Let $\sum_{m=1}^{N_{i-total}} \varepsilon_{i_m}$, $\sum_{m=1}^{N_{i-total}} RE_{i_m}$, and $\sum_{m=1}^{N_{i-total}} E_{i_m}^{use}$ denote the initial energy of total sensor nodes in corona C_i, the residual energy of total sensor nodes in corona C_i, and the energy used of the sensor nodes in corona C_i, respectively.

According to the energy conservation law, energy used of total sensor nodes is equivalent to initial energy of total sensor nodes minus residual energy of total sensor nodes. Therefore, $\sum_{m=1}^{N_{i-total}} E_{i_m}^{use} = \sum_{m=1}^{N_{i-total}} \varepsilon_{i_m} - \sum_{m=1}^{N_{i-total}} RE_{i_m}, \forall i$.

Our objective is to achieve maximum throughput. That is, $Max \sum_{m=1}^{N_{i-total}} E_{i_m}^{use}, \forall i$. Once a sensor node is exhausted, the sensed data of the other sensor nodes may not be delivered to the sink node, resulting in a waste of energy. In order to avoid this scenario, it needs to be satisfied $\sum_{m=1}^{N_{i-total}} RE_{i_m} = 0$, $\forall i$, which represents that each sensor node use up its energy at approximately the same time. In other words, $\sum_{m=1}^{N_{i-total}} E_{i_m}^{use} = \sum_{m=1}^{N_{i-total}} \varepsilon_{i_m}, \forall i$. Hence, we prove that balancing the energy consumption can achieve maximum throughput.

Theorem 4.2: Within each corona, balancing the energy consumption among sensor nodes can achieve maximum network lifetime.

Proof: First, we form the contrapositive of the given statement. That is, if the maximum network lifetime cannot be achieved, then balanced energy consumption is not held.

Now, we suppose that the maximum network lifetime cannot be achieved. By definition of it (i.e., maximum network lifetime cannot be achieved), we have $\frac{\sum_{m=1}^{N_{i-total}} E_{im}^{use}}{Total_{Ei}} < \frac{\sum_{m=1}^{N_{i-total}} \varepsilon_{im}}{Total_{Ei}}$, where $\mathrm{Total_{Ei}}$ is the total energy consumption of CHs in the corona $\mathrm{C_i}$. In other words, $\sum_{m=1}^{N_{i-total}} RE_{i_m} > 0$. This equation also means that sensor nodes cannot use up their energy at approximately the same time (i.e., balanced energy consumption is not held). This completes the proof.

Theorem 4.3: Balanced energy consumption is impossible when $\mathrm{r_i} = \mathrm{r_j}$, $\varepsilon_\mathrm{i} = \varepsilon_\mathrm{j}$ and $\mathrm{DA_i} = \mathrm{DA_j}$, $\forall i, j,\ i \neq j$.

Proof: (By contradiction) We assume that it is possible to achieve balanced energy consumption when $\mathrm{r_i} = \mathrm{r_j}$ and $\varepsilon_\mathrm{i} = \varepsilon_\mathrm{j}$, $\forall i, j, i \neq j, 1 \leq i, j \leq k$, where k is the number of coronas. Based on Definition 3.4,

$$\frac{N_1 \times \varepsilon_1}{E_1} = \frac{N_2 \times \varepsilon_2}{E_2} = \cdots = \frac{N_{i-1} \times \varepsilon_{i-1}}{E_{i-1}} = \frac{N_i \times \varepsilon_i}{E_i}.$$

Basically, each CH ($\mathrm{CH_{i,j}}$) in the outermost corona $\mathrm{C_k}$ only needs to transmit data generated by its own cluster members; however, each CH in corona $\mathrm{C_{k-1}}$ not only handles the data transmitted by its own cluster members but also relays packets from corona $\mathrm{C_k}$. Therefore, we discuss the case for sensor nodes in the two outermost coronas: corona $\mathrm{C_{k-1}}$ and corona $\mathrm{C_k}$.

$$\frac{N_{k-1} \times \varepsilon_{k-1}}{E_{k-1}} = \frac{N_k \times \varepsilon_k}{E_k} \tag{5}$$

Applying (4) to (5), (5) can be rewritten into

$$\frac{N_{k-1} \times \varepsilon_{k-1}}{[N_{k-1} + N_k \times \frac{a_k}{a_{k-1}}] \times [E_{elec} + E_{amp} \times (r_{k-1} + r_{k-2})^n]} = \frac{N_k \times \varepsilon_k}{N_k \times [E_{elec} + E_{amp} \times (r_k + r_{k-1})^n]} \tag{6}$$

Because of $\mathrm{r_{k-1}} = \mathrm{r_{k-2}} = \mathrm{r_k}$ and $\varepsilon_{\mathrm{k-1}} = \varepsilon_\mathrm{k}$, we have

$$\frac{N_{k-1}}{[N_{k-1} + N_k \times \frac{a_k}{a_{k-1}}]} = \frac{N_k}{N_k} = 1. \tag{7}$$

Leading to

$$N_{k-1} + N_k \times \frac{a_k}{a_{k-1}} = N_{k-1}. \tag{8}$$

Finally, we obtain

$$N_k \times \frac{a_k}{a_{k-1}} = 0. \tag{9}$$

(9) indicates that CHs in the outermost corona $\mathrm{C_k}$ cannot transmit any data to corona $\mathrm{C_{k-1}}$, which is impractical. Consequently, the proof of this theorem is completed.

Theorem 4.4: When $\mathrm{r_1} = \mathrm{r_2} = \ldots = r_{\mathrm{k-1}} = \mathrm{r_k}$, $\varepsilon_1 = \varepsilon_2 = \ldots = \varepsilon_{\mathrm{k-1}}$ and $\mathrm{DA_k} = \mathrm{DA_{k-1}}$, nearly balanced energy (BE) consumption of the whole network is achievable if

$$0 < \frac{\varepsilon_k}{\varepsilon_{k-1}} = \frac{N_{k-1}}{N_{k-1} + N_k \times \frac{a_k}{a_{k-1}}} < 1.$$

Proof: We begin by showing that if BE holds, then $0 < \frac{\varepsilon_k}{\varepsilon_{k-1}} = \frac{N_{k-1}}{N_{k-1} + N_k \times \frac{a_k}{a_{k-1}}} < 1$. For the case when $\mathrm{r_1} = \mathrm{r_2} = \ldots = \mathrm{r_{k-1}} = \mathrm{r_k}$ and $\varepsilon_1 = \varepsilon_2 = \ldots = \varepsilon_{\mathrm{k-1}} \neq \varepsilon_\mathrm{k}$. Applying (4) to (5), we rewrite (5) as

$$\frac{N_{k-1} \times \varepsilon_{k-1}}{[N_{k-1} + N_k \times \frac{a_k}{a_{k-1}}] \times [E_{elec} + E_{amp} \times (r_{k-1} + r_{k-2})^n]} = \frac{N_k \times \varepsilon_k}{N_k \times [E_{elec} + E_{amp} \times (r_k + r_{k-1})^n]} \tag{10}$$

After simplification, we obtain

$$\frac{N_{k-1}}{[N_{k-1} + N_k \times \frac{a_k}{a_{k-1}}]} = \frac{\varepsilon_k}{\varepsilon_{k-1}} = p. \tag{11}$$

For convenience, we denote $\frac{\varepsilon_k}{\varepsilon_{k-1}}$ as p. Because $N_k \times \frac{a_k}{a_{k-1}} > 0$, nearly balanced energy consumption is achievable if

$$0 < p = \frac{\varepsilon_k}{\varepsilon_{k-1}} = \frac{N_{k-1}}{N_{k-1} + N_k \times \frac{a_k}{a_{k-1}}} < 1. \tag{12}$$

This completes the proof of the first half.

Then, we prove that if $0 < \frac{\varepsilon_k}{\varepsilon_{k-1}} = \frac{N_{k-1}}{N_{k-1} + N_k \times \frac{a_k}{a_{k-1}}} < 1$, nearly balanced energy consumption of the whole network is achievable (i.e., BE holds).

$$\text{Because } 0 < \frac{\varepsilon_k}{\varepsilon_{k-1}} = \frac{N_{k-1}}{N_{k-1} + N_k \times \frac{a_k}{a_{k-1}}} < 1,$$
$$\frac{N_k \times \varepsilon_k}{N_k} = \frac{N_{k-1} \times \varepsilon_{k-1}}{(N_{k-1} + N_k \times \frac{a_k}{a_{k-1}})}. \tag{13}$$

Because of $\mathrm{r_1} = \mathrm{r_2} = \ldots = \mathrm{r_{k-1}} = \mathrm{r_k}$, we have

$$[E_{elec} + E_{amp} \times (r_k + r_{k-1})^n] = [E_{elec} + E_{amp} \times (r_{k-1} + r_{k-2})^n]. \tag{14}$$

(13) can be rewritten as

$$\frac{N_k \times \varepsilon_k}{N_k \times [E_{elec} + E_{amp} \times (r_k + r_{k-1})^n]} = \frac{N_{k-1} \times \varepsilon_{k-1}}{(N_{k-1} + N_k \times \frac{a_k}{a_{k-1}}) \times [E_{elec} + E_{amp} \times (r_{k-1} + r_{k-2})^n]} \tag{15}$$

Finally, we get $\frac{N_k \times \varepsilon_k}{E_k} = \frac{N_{k-1} \times \varepsilon_{k-1}}{E_{k-1}}$ (i.e., BE holds). Therefore, the proof of the theorem is completed.

Corollary 4.5: Given a_{k-1} and a_k, nearly balanced energy (BE) consumption is achievable if

$$0 < \frac{\rho_{k-1} \times a_{k-1}}{\rho_k \times a_k + \rho_{k-1} \times a_{k-1}} < 1,$$

$r_1 = r_2 = \ldots = r_{k-1} = r_k$ and $\varepsilon_1 = \varepsilon_2 = \ldots = \varepsilon_{\mathrm{k-1}} \neq \varepsilon_\mathrm{k}$.

Proof: We first show that, if BE holds, then $0 < \frac{\rho_{k-1} \times a_{k-1}}{\rho_k \times a_k + \rho_{k-1} \times a_{k-1}} < 1$. From (11), we get

$$p \times N_{k-1} + p \times N_k \times \frac{a_k}{a_{k-1}} = N_{k-1}. \tag{16}$$

After basic transformations, we have

$$\frac{1-p}{p} = \frac{N_k}{N_{k-1}} \times \frac{a_k}{a_{k-1}}. \tag{17}$$

For the same reason as in the proof of Theorem 4.4, substituting N_k and N_{k-1} in (3) into (17), we obtain

$$\frac{1-p}{p} = \frac{\pi \times r_k^2 \times \rho_k}{\pi \times r_{k-1}^2 \times \rho_{k-1}} \times \frac{a_k}{a_{k-1}} \tag{18}$$

And, consequently,

$$\frac{1-p}{p} = \frac{\rho_k}{\rho_{k-1}} \times \frac{a_k}{a_{k-1}}. \tag{19}$$

The above equation can be rewritten as $\frac{1-p}{p} = q$, where

$$q = \frac{\rho_k}{\rho_{k-1}} \times \frac{a_k}{a_{k-1}}. \tag{20}$$

Leading to

$$p = \frac{1}{q+1} = \frac{\varepsilon_k}{\varepsilon_{k-1}}. \tag{21}$$

According to (12), we have

$$0 < \frac{1}{q+1} < 1. \tag{22}$$

Finally, we obtain $0 < \frac{\rho_{k-1} \times a_{k-1}}{\rho_k \times a_k + \rho_{k-1} \times a_{k-1}} < 1$. It completes the proof of the first half.

The reverse implication can be shown similarly. Hence, this concludes the proof (note that the value of $\rho_i, \forall i = 1 \cdots k$ must be a positive number, as calculated later in Section V.C).

V. PROPOSED SCHEMES

The proposed END-BE and END-MLT schemes consist of three phases: network initialization phase, cluster formation phase, and data routing phase. The main difference between END-BE and END-MLT is that END-MLT has the same initial energy of each sensor node, including sensor nodes in the outermost corona (i.e., $\varepsilon_1 = \varepsilon_2 = \ldots = \varepsilon_{k-1} = \varepsilon_k = 1$ joule), while END-BE does not (i.e., $\varepsilon_1 = \varepsilon_2 = \ldots = \varepsilon_{k-1} = 1 \neq \varepsilon_k$). This case may lead to different node deployment results in each corona. In short, the main objective of END-BE is to achieve balanced energy consumption among sensor nodes, and that of END-MLT is to extend network lifetime.

A. NETWORK INITIALIZATION PHASE

The network initialization phase consists of determining the total radius of the topology and calculating the node density in each corona.

• *Determining the Total Radius of the Topology (R)*

In this model, the width of each corona is set to w. Therefore,

$$r_i = \frac{w}{2}, \quad \forall i = 1 \cdots k. \tag{23}$$

Once the number of coronas (k) is determined, the total radius of the topology is obtained accordingly. Note that the number of coronas (k) can be determined based on the delay tolerance value of user requirements. The higher number of coronas, the larger hop counts the sensed data need to be transmitted. Thus, the delay is increased. On the other hand, when the number of coronas is small, delay can be decreased.

• *Calculating the Node Density in each Corona (for **END-BE**Scheme)*

We assume that all sensor nodes are deployed *a priori* and the number of sensor nodes in the coronas satisfies the following conditions:

$$\frac{[\pi \times (r_1)^2 \times \rho_1] \times \varepsilon_1}{E_1} \approx \frac{[\pi \times (r_2)^2 \times \rho_2] \times \varepsilon_2}{E_2} \approx \ldots \approx \frac{[\pi \times (r_i)^2 \times \rho_i] \times \varepsilon_i}{E_i}, \quad \forall i = 1 \cdots k. \tag{24a, 24b}$$

$$\sum_{i=1}^{k} a_i \times [\pi \times (r_i)^2 \times \rho_i] = N_{ALL} \tag{24c}$$

$$\text{subject to: } N_{i-\text{total}} \geq a_i, \quad \forall i = 1 \cdots k, \tag{24d}$$

where r_i and ρ_i are the cluster radius and the node density in corona C_i, respectively, ε_i is the initial energy of each sensor node in corona C_i (i.e., $\varepsilon_1 = \varepsilon_2 = \ldots = \varepsilon_{k-1} = 1$ joule and an adjustable ε_k), E_i is the total energy consumption of each CH in corona C_i [as mentioned in (4)], a_i is the number of clusters in C_i, N_{ALL} is the total number of sensor nodes (note that this parameter is flexible in our scheme), and $N_{i-\text{total}}$ is the total number of sensor nodes in corona i ($N_{i-\text{total}} = a_i \times [\pi \times (r_i)^2 \times \rho_i]$, $1 \leq i \leq k$). We can calculate the ratio of $\rho_1, \rho_2, \ldots, \rho_i$ via (24a). From (24a) and (24c), we then know how many sensor nodes should be deployed into each corona. Constraint (24c) ensures that each cluster environment is completely covered by at least one sensor node. Accordingly, $\rho_i \geq \frac{1}{\pi \times (r_i)^2}, \forall i = 1 \cdots k$.

• *Calculating the Node Density in each Corona (for **END-MLT** Scheme)*

The node deployment strategy satisfies the following conditions:

$$\frac{[\pi \times (r_1)^2 \times \rho_1] \times \varepsilon_1}{E_1} \approx \frac{[\pi \times (r_2)^2 \times \rho_2] \times \varepsilon_2}{E_2} \approx \ldots \approx \frac{[\pi \times (r_{k-1})^2 \times \rho_{k-1}] \times \varepsilon_{k-1}}{E_{k-1}} \tag{25a}$$

$$\rho_k \leftarrow \frac{1}{\pi \times (r_k)^2} \tag{25b}$$

$$\sum_{i=1}^{k-1} a_i \times [\pi \times (r_i)^2 \times \rho_i] = N_{ALL} - [a_k \times \pi \times (r_k)^2 \times \rho_k] \tag{25c}$$

$$\text{subject to: } N_{i-\text{total}} \geq a_i, \forall i = 1 \cdots K - 1. \tag{25d}$$

(25a) balances energy consumption among sensor nodes in coronas C_1 to C_{k-1} (excluding the outermost corona C_k). From (25b), ρ_k is the node density in corona C_k, which means that we first assign a_k nodes in the outermost corona when we implement END-MLT (i.e., it deploys 24, 48, 48, and 48

sensor nodes in the outermost corona when $R = 300\ m$, $400\ m$, $500\ m$, and $600\ m$, respectively). Specifically, the END-MLT scheme first arranges one sensor node for each cluster in the outermost corona. From (25a) to (25c), we can find out how many sensor nodes should be deployed for each corona. Constraint (25d) ensures that each cluster environment is completely covered by at least one sensor node.

Based on the above statement, four differences between END-BE and END-MLT in network initialization phase are listed as follows:

1) **Difference in ε_i:** In END-BE scheme, initial energy of each sensor node in coronas C_1 to C_{k-1} is the same, while initial energy of each sensor node in the outermost corona C_k is adjustable (i.e., $\varepsilon_1 = \varepsilon_2 = \ldots = \varepsilon_{k-1} = 1$ joule and an adjustable ε_k). Nevertheless, END-MLT has the same initial energy of each sensor node, including sensor nodes in the outermost corona (i.e., $\varepsilon_1 = \varepsilon_2 = \ldots = \varepsilon_{k-1} = \varepsilon_k = 1$ joule).

2) **Difference in balanced requirements:** The END-BE scheme pursues the goal of balanced energy consumption among all coronas [as shown in (24a)]. However, the objective of END-MLT is to achieve balanced energy consumption among coronas C_1 to C_{k-1}, excluding the outermost corona C_k [as shown in (25a)].

3) **Difference in deployment strategies:** END-BE scheme simultaneously deploys sensor nodes in all coronas according to computational result of (24a) and (24c). In END-MLT scheme, it first deploys a_k sensor nodes in the outermost corona [as shown in (25b)], and then remaining sensor nodes are assigned to coronas C_1 to C_{k-1} [as shown in (25c)].

4) **Difference in objectives:** The main goal of END-BE is to achieve balanced energy consumption among sensor nodes, and that of END-MLT is to achieve longer network lifetime.

• *A Numerical Example (for **END-BE** Scheme)*

Consider an example of the four-corona model with $R = 400\ m$. Therefore, $r_i = \frac{100}{2} = 50m$, $\forall i = 1 \cdots 4$. In order to achieve a fair comparison, the total number of sensor nodes is determined based on the q-switch model in [18] for later comparisons (i.e., we deploy 216 sensor nodes in the topology).

Given $\varepsilon_1 = \varepsilon_2 = \varepsilon_3 = 1$ joule and an adjustable ε_4 (i.e., 0.4), the ratio of ρ_1, ρ_2, ρ_3, and ρ_4 can be obtained by (26a). The obtained ratio can be put in (26b) to calculate the number of sensor nodes in each corona with the goal of achieving nearly balanced energy consumption.

$$\frac{[\pi \times (50)^2 \times \rho_1] \times 1}{E_1} \approx \frac{[\pi \times (50)^2 \times \rho_2] \times 1}{E_2} \approx \frac{[\pi \times (50)^2 \times \rho_3] \times 1}{E_3} \approx \frac{[\pi \times (50)^2 \times \rho_4] \times \varepsilon_4}{E_4} \quad (26a)$$

$$4 \times [\pi(50)^2 \times \rho_1] + 12 \times [\pi(50)^2 \times \rho_2] + 24 \times [\pi(50)^2 \times \rho_3] + 48 \times [\pi(50)^2 \times \rho_4] = 216 \quad (26b)$$

$$\text{subject to: } N_{i-\text{total}} \geq a_i, \forall i = 1 \cdots 4, \quad (26c)$$

where E_i is the total energy consumption of each CH in corona C_i, $i = 1 \ldots 4$ (as stated in Section IV.A).

TABLE 2. The number of sensor nodes deployed in each corona.

K-Corona Model \ N_i		$N_{1\text{-total}}$ a_1=4	$N_{2\text{-total}}$ a_2=12	$N_{3\text{-total}}$ a_3=24	$N_{4\text{-total}}$ a_4=48	$N_{5\text{-total}}$ a_5=48	$N_{6\text{-total}}$ a_6=48
3-Corona Model R=300, N=72	ε_k=0.2	5	13	54	×	×	×
	ε_k=0.4	9	25	38	×	×	×
	ε_k=0.6	14	35	23*	×	×	×
	ε_k=0.8	18	43	11*	×	×	×
4-Corona Model R=400, N=216	ε_k=0.2	14	41	32	129	×	×
	ε_k=0.4	28	75	45	68	×	×
	ε_k=0.6	42	104	42	28*	×	×
	ε_k=0.8	56	128	26	6*	×	×
5-Corona Model R=500, N=648	ε_k=0.2	42	121	97	78	310	×
	ε_k=0.4	84	226	135	81	122	×
	ε_k=0.6	126	313	125	50	34*	×
	ε_k=0.8	167	385	77	15*	4*	×
6-Corona Model R=600, N=1944	ε_k=0.2	125	364	291	233	186	745
	ε_k=0.4	251	677	406	244	146	220
	ε_k=0.6	377	940	376	151	60	40*
	ε_k=0.8	502	1154	231	46*	9*	2*

From the above equations, we get $\rho_1 \approx 0.000888535$, $\rho_2 \approx 0.000798726$, $\rho_3 \approx 0.000239618$, and $\rho_4 \approx 0.000179713$. Accordingly, $N_{1-\text{total}} = 28$, $N_{2-\text{total}} = 75$, $N_{3-\text{total}} = 45$ and $N_{4-\text{total}} = 68$. It is easy to extend this example to the K-corona model, as shown in Table 2. The superscript * is used to explicitly denote that Constraint (26c) is not held.

B. CLUSTER FORMATION PHASE

END-BE and END-MLT schemes are the same in the cluster-formation phase and data-forwarding phase. Hence, we will not describe them separately. The cluster-formation phase consists of cluster setup and CH rotation in a cluster.

• *Cluster Setup*

The base station (BS) first selects a_i sensor nodes in corona C_i to serve as CHs. In other words, BS selects four CHs in corona C_1, 12 CHs in corona C_2, 24 CHs in corona C_3 due to $a_1 = 4$, $a_2 = 12$, $a_3 = 24$, etc. The selected CH broadcasts a Head_Msg. This message includes current residual energy, the distance to the sink, and the sensor node's ID, which is used as the cluster's ID as well. If two or more Head_Msgs are broadcasted to a sensor node, it only joins the closest CH before sending a Member_Msg to notify the CH of its condition. For a sensor node that does not serve as the CH and does not receive any Head_Msg from the CHs, a sensor node may send a Find_Msg to seek the closest cluster to join.

• *CH Rotation within the Cluster*

The CH rotation is important due to the fact that the relay loads imposed on the CHs may be larger than those on the sensor nodes. In order to uniformly distribute energy consumption among all sensor nodes, this phase defines the threshold of CH energy as T. If the residual power of current

CH is under T, BS reselects an appropriate number of sensor nodes (with most residual energy) in corona C_i to serve as new CHs (e.g., BS reselects four sensor nodes in corona C_1, 12 in C_2, 24 in C_3 due to $a_1 = 4$, $a_2 = 12$, $a_3 = 24$, etc), while the Change_Msg are broadcasted by each new CH to notice its members of changing the CH.

C. DATA FORWARDING PHASE

It is well known that the energy consumed in a radio transmission can be proportional to the fourth power of transmission range. If the sensor node utilizes single-hop routing to transmit data to the CH, then the sensor node farthest from the CH uses up much more energy. In view of this fact, intra-cluster data routing employs the concept of the minimum spanning tree (MST) [20]. The purpose is to reduce the transmission distance between sensor nodes and CHs. Afterward, sensor nodes transmit the sensed data to their designated CH. All CHs in corona C_i perform inter-cluster data routing and then transmit the received data via the next CHs in corona C_{i-1}. Finally, let us specify how CH-to-CH transmission capacity can be obtained.

We know that the relaying capacity (S_{i-1}) of the CH in corona C_{i-1} from CHs in corona C_i is

$$S_{i-1} = \frac{a_i}{a_{i-1}} \times M_i = \frac{8i-4}{8(i-1)-4} \times M_i, \forall i = 2 \ldots k, \tag{27}$$

where M_i is the messages transferred by a CH at corona C_i, and a_i is the number of clusters in corona C_i (as mentioned before in (2)).

For example, 12 clusters are in corona C_2 (i.e., $a_2 = 12$) and four clusters are in corona C_1 (i.e., $a_1 = 4$). It is easily understood that each CH in corona C_1 has relaying capacity of $\frac{12}{4} \times M_2$ from CHs in corona C_2, where M_2 are the messages transferred by a CH at corona C_2. In addition, the logical partition of clusters in each corona is further considered for the purpose of load balancing (as mentioned earlier in Section III.A); that is, the ratio of a_{i-1} to a_i is an integer, $\forall i = 2 \cdots k$. It also indicates that the relaying capacity delivered from CHs in corona C_i is equally shared by CHs in corona C_{i-1}.

VI. SIMULATIONS

In this section, we evaluate and compare END-BE, END-MLT, q-switch scheme [18], and Uniform scheme, which sensor nodes are distributed uniformly in the sensing area. We also assume the ideal scenario, which only considers a perfect MAC layer to resolve wireless channel issues [6]. The following parameters are used to compare all of these schemes.

$E_{elec} = 50$ nJ/bit, $\varepsilon_{amp} = 0.0013$ pJ/bit/m ^{4}, the path loss exponent is 4; initial energy of each sensor node is 1 joule (except for END-BE); the sensing range of each sensor node is 50 meters; each sensor node sends 400 bits of data per unit time to the sink via multihop communications. In order to achieve a fair comparison, the data aggregation ratio is set to 1. We averaged the results of 200 runs for each scenario. We then compared the performance metrics with the cluster coverage rate, network lifetime, and residual energy. "Network lifetime" is defined as the elapsing time until the first sensor node uses up its energy and is measured in "rounds." The definition of a "round" is that one packet is transferred from the sensor node via the CHs to the sink.

TABLE 3. The deployed results under different schemes.

K-Corona Model	N_i	$N_{1\text{-total}}$ a_1=4	$N_{2\text{-total}}$ a_2=12	$N_{3\text{-total}}$ a_3=24	$N_{4\text{-total}}$ a_4=48	$N_{5\text{-total}}$ a_5=48	$N_{6\text{-total}}$ a_6=48
3-Corona Model	q-switch	48	16	8	×	×	×
R=300,	END-BE	9	25	38	×	×	×
N=72	END-MLT	14	34	24	×	×	×
4-Corona Model	q-switch	144	48	16	8	×	×
R=400,	END-BE	28	75	45	68	×	×
N=216	END-MLT	34	89	45	48	×	×
5-Corona Model	q-switch	432	144	48	16	8	×
R=500,	END-BE	84	226	135	81	122	×
N=648	END-MLT	115	294	132	59	48	×
6-Corona Model	q-switch	1296	432	144	48	16	8
R=600,	END-BE	251	677	406	244	146	220
N=1944	END-MLT	366	919	384	160	67	48

A. COVERAGE RATE

We first evaluate the END-MLT, END-BE, q-switch scheme, and the Uniform scheme in terms of the coverage rate. In order to achieve a fair comparison, the total number of sensor nodes is determined based on the q-switch model in [18] (i.e., it deploys 72, 216, 648, 1944 sensor nodes in the area of $R = 300\ m$, $400\ m$, $500\ m$, and $600\ m$, respectively). For END-BE under $R = 300\ m$ to $600\ m$, the initial energy (ε_k) of each sensor node in the outermost corona is set to 0.4. The reason why we do not choose 0.2, 0.6, or 0.8 is as follows. If we choose 0.2, then sensor nodes are crowded into the outermost corona (as previously mentioned in Table 2); if we choose 0.6 or 0.8, then some cases may not fit the constraint condition (i.e., see the superscript *, as shown in Table 2). The deployed sensor nodes in each corona of END-MLT and END-BE need to be calculated based on (24a-c) and (25a-d) using the given parameters. In the Uniform scheme, the node distribution strategy is to uniformly distribute sensor nodes in the sensing field. All of the deployed results in each corona are shown in Table 3.

For the case of the END-BE scheme in the three-corona model, BS selects four CHs in corona C_1, 12 CHs in corona C_2, and 24 CHs in corona C_3. These selected CHs broadcast Head_Msg. The remaining sensor nodes in each corona can join the closest CH. Specifically, the remaining number of sensor nodes are five in corona C_1, 13 in corona C_2, and 14 in corona C_3 (i.e., 9–4 = 5, 25–12 = 13, 38–24 = 14). Once the residual power of current CH is under T, BS reselects sensor nodes with the most residual energy to serve as new CHs, while the Change_Msg are broadcasted to note the change of the CH, as mentioned earlier in Section V.B. Therefore, the energy consumption can be shared by each sensor node.

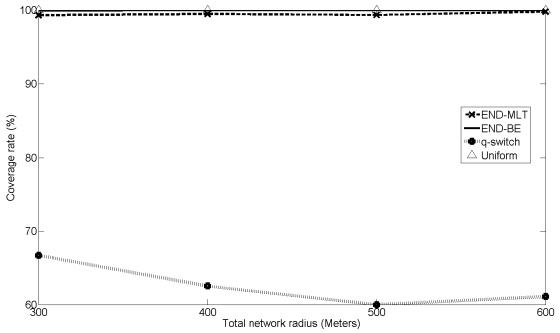

FIGURE 2. Cluster coverage rate for different schemes in the initial deployment scenario.

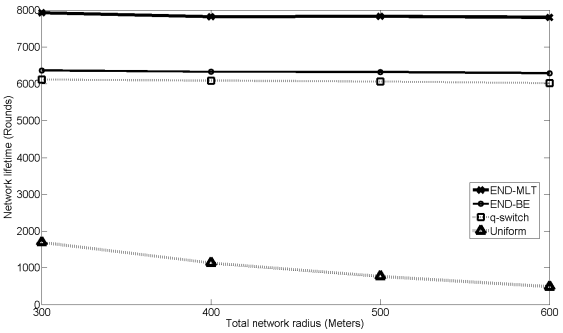

FIGURE 3. Network lifetime of different schemes.

Figure 2 shows the cluster coverage rate of the initial deployment scenario for END-MLT, END-BE, q-switch, and Uniform schemes. Coverage rate is defined as the ratio of coverage area to total cluster area. Here, it can be observed that the cluster coverage rate of the END-MLT scheme is over 99%. In addition, the coverage rate of END-BE is near 100%. The reason for these results is due to deployment approaches (as mentioned in 24c and 25d). We can see that the cluster coverage rate of the q-switch scheme is only between 60 and 66.6%. These values can be explained by the fact that the q-switch scheme only deploys eight sensor nodes in the outermost corona for each scenario. Some regions cannot be covered, especially for the outermost corona C_k and C_{k-1}. Thus, the coverage rate is lowest. As for the Uniform scheme, the node distribution strategy is to uniformly distribute sensor nodes in the sensing field. Therefore, the coverage rate is highest (i.e., about 100%).

B. NETWORK LIFETIME

Figure 3 clearly shows the performance improvement of END-MLT compared with END-BE, q-switch, and Uniform schemes in terms of network lifetime. END-MLT matches the design goal of having a longer network lifetime. This is because END-MLT uses an energy-balanced node-deployment algorithm with $\varepsilon_k = 1$ joule; meanwhile, END-BE with $\varepsilon_k = 0.4$ joule (END-BE has an energy-balanced objective, as discuss in Section VI.C). As for the q-switch scheme, their basic idea is that each sensor node sends its data to one of the adjacent inner neighbors with maximum residual energy (thus, extra route-selection overhead per round is needed). Compared with the q-switch scheme, END-MLT and END-BE aim at that each cluster is completely covered by at least one sensor node [as mentioned in (24c) and (25d)]. END-MLT and END-BE further adopt the proposed energy-balanced node deployment algorithm. In addition, they also use the cluster technique to reduce the energy consumption. As expected, the Uniform scheme has the worst network lifetime of the four schemes.

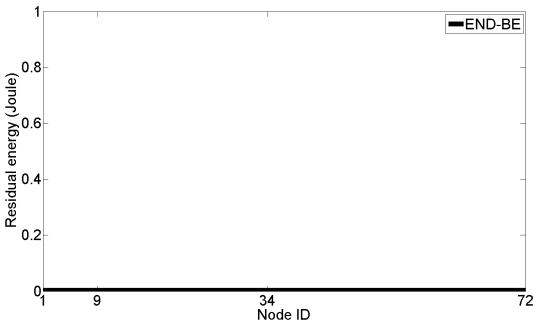

FIGURE 4. Residual energy of 72 sensor nodes in the END-BE scheme.

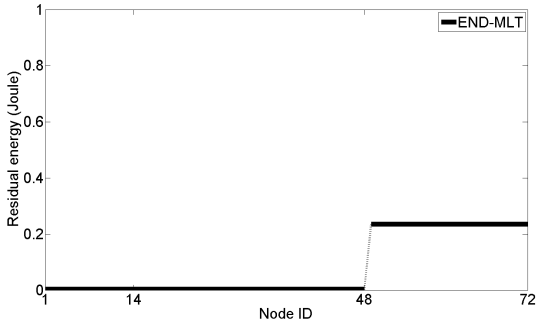

FIGURE 5. Residual energy of 72 sensor nodes in the END-MLT scheme.

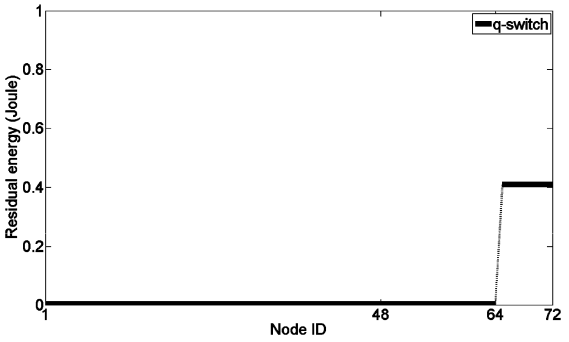

FIGURE 6. Residual energy of 72 sensor nodes in the q-switch scheme.

C. RESIDUAL ENERGY

To evaluate the proposed END-BE and END-MLT schemes in terms of residual energy, we compared them with the q-switch and Uniform schemes for the three- and four-corona models. Figures 4–7 show the residual energy of each sensor

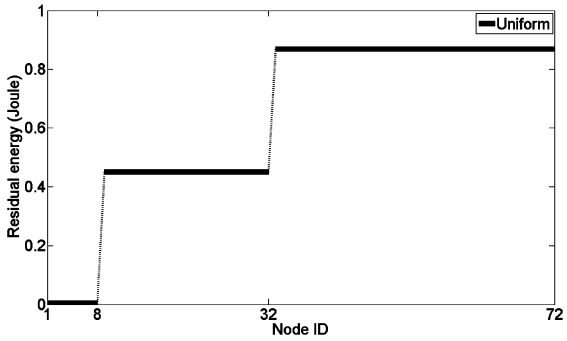

FIGURE 7. Residual energy of 72 sensor nodes in the Uniform scheme.

node for the four strategies when the network operation ends. Note that 72 sensor nodes are assigned IDs starting from the innermost corona to the outermost corona. The network radius is set to 300 m.

Figures 4–7 show that most sensor nodes use up their energy nearly at the same time when utilizing our END-BE. As a matter of fact, the residual energy for most of the sensor nodes is less than 3.95×10^{-3} joule. That is, energy balance in each corona is indeed achieved. It is easy to understand that the Uniform scheme has a large quantity of residual energy unused from the innermost corona to the outermost corona, especially for sensor nodes in the outermost corona (i.e., 88% of initial energy remains unused). As for END-MLT, we observe that a large amount of residual energy remains unused in sensor nodes in the outermost corona (C_3). Besides, most of the sensor nodes in coronas C_1 to C_2 almost exhaust their energy when the network operation terminates. This is consistent with our expectation. The same result is obtained in the q-switch scheme. In other words, the energy consumption is not well-balanced for all coronas in the q-switch scheme. The same trends are for the four-corona model (results are not shown due to space limitations). Therefore, we can conclude that our END-BE scheme is more energy-balanced than the END-MLT, q-switch and Uniform schemes.

VII. CONCLUSIONS AND FUTURE WORKS

In a corona-based WSN, CHs closer to the sink are loaded more than those farther from it. To overcome this situation, we propose END-BE, which adjusts the initial energy of sensor nodes in the outermost corona. Based on the analysis, we can calculate how many sensor nodes should be deployed into each corona, so that each cluster can use up its energy at approximately the same time. We also propose END-MLT, which further lengthens the network lifetime by arranging appropriate sensor nodes (with $\varepsilon_k = 1$) in the outermost corona with the goal of balancing the energy consumption in coronas C_1 to C_{k-1}. Simulation results show that energy consumption is nearly balanced by implementing END-BE, and the network lifetime is greatly improved by adopting END-MLT.

As to future work, we will investigate the energy-balanced node deployment scheme for other models, such as areas with irregular shapes and situations where the sink is located at different places. In addition, what is the best value of ε_k? The parameter can be further investigated as well.

REFERENCES

[1] X. Tan, Z. Sun, and I. F. Akyildiz, "Wireless underground sensor networks: MI-based communication systems for underground applications," *IEEE Antennas Propag. Mag.*, vol. 57, no. 4, pp. 74–87, Aug. 2015.
[2] J. Li, Q.-S. Jia, X. Guan, and X. Chen, "Tracking a moving object via a sensor network with a partial information broadcasting scheme," *Inf. Sci.*, vol. 181, no. 20, pp. 4733–4753, 2011.
[3] L. V. Nguyen, S. Kodagoda, R. Ranasinghe, and G. Dissanayake, "Information-driven adaptive sampling strategy for mobile robotic wireless sensor network," *IEEE Trans. Control Syst. Technol.*, vol. 24, no. 1, pp. 372–379, Jan. 2016.
[4] S. Misra, S. Mishra, and M. Khatua, "Social sensing-based duty cycle management for monitoring rare events in wireless sensor networks," *IET Wireless Sensor Syst.*, vol. 5, no. 2, pp. 68–75, 2015.
[5] P. Chanak, I. Banerjee, and R. S. Sherratt, "Simultaneous mobile sink allocation in home environments with applications in mobile consumer robotics," *IEEE Trans. Consum. Electron.*, vol. 61, no. 2, pp. 181–188, May 2015.
[6] J. Li and P. Mohapatra, "An analytical model for the energy hole problem in many-to-one sensor networks," in *Proc. IEEE Veh. Technol. Conf.*, Sep. 2005, pp. 2721–2725.
[7] H. M. Ammari, "Investigating the energy sink-hole problem in connected k-covered wireless sensor networks," *IEEE Trans. Comput.*, vol. 63, no. 11, pp. 2729–2742, Nov. 2014.
[8] S. Olariu and I. Stojmenovic, "Design guidelines for maximizing lifetime and avoiding energy holes in sensor networks with uniform distribution and uniform reporting," in *Proc. Int. Conf. Comput. Commun.*, 2006, pp. 1–12.
[9] C.-Y. Chang, C.-Y. Chang, Y.-C. Chen, and H.-R. Chang, "Obstacle-resistant deployment algorithms for wireless sensor networks," *IEEE Trans. Veh. Technol.*, vol. 58, no. 6, pp. 2925–2941, Jul. 2009.
[10] S. Halder and A. Ghosal, "A location-wise predetermined deployment for optimizing lifetime in visual sensor networks," *IEEE Trans. Circuits Syst. Video Technol.*, vol. 26, no. 6, pp. 1131–1145, Jun. 2016.
[11] M. Rout and R. Roy, "Self-deployment of mobile sensors to achieve target coverage in the presence of obstacles," *IEEE Sensors J.*, vol. 16, no. 14, pp. 5837–5842, Jul. 2016.
[12] S. C. Ergen and P. Varaiya, "Optimal placement of relay nodes for energy efficiency in sensor networks," in *Proc. IEEE Int. Conf. Commun.*, Jun. 2006, pp. 3473–3479.
[13] I. Howitt and J. Wang, "Energy balanced chain in distributed sensor networks," in *Proc. Wireless Commun. Netw. Conf.*, vol. 3. 2004, pp. 1721–1726.
[14] A. Ababnah and B. Natarajan, "Optimal control-based strategy for sensor deployment," *IEEE Trans. Syst., Man, Cybern. A, Syst., Humans*, vol. 41, no. 1, pp. 97–104, Jan. 2011.
[15] J. Lian, K. Naik, and G. B. Agnew, "Data capacity improvement of wireless sensor networks using non-uniform sensor distribution," *Int. J. Distrib. Sensor Netw.*, vol. 2, no. 2, pp. 121–145, Apr./Jun. 2006.
[16] Y. Liu, H. Ngan, and L. M. Ni, "Power-aware node deployment in wireless sensor networks," *Int. J. Distrib. Sensor Netw.*, vol. 3, pp. 225–241, Apr. 2007.
[17] S. Olariu and I. Stojmenović, "Data-centric protocols for wireless sensor networks," in *Handbook of Sensor Networks: Algorithms and Architectures*. Hoboken, NJ, USA: Wiley, 2005, pp. 417–456.
[18] X. Wu, G. Chen, and S. K. Das, "Avoiding energy holes in wireless sensor networks with nonuniform node distribution," *IEEE Trans. Parallel Distrib. Syst.*, vol. 19, no. 5, pp. 710–720, May 2008.
[19] W. B. Heinzelman, A. P. Chandrakasan, and H. Balakrishnan, "An application-specific protocol architecture for wireless microsensor networks," *IEEE Trans. Wireless Commun.*, vol. 1, no. 4, pp. 660–670, Oct. 2002.
[20] H. Shen, "Finding the k most vital edges with respect to minimum spanning tree," *Acta Inf.*, vol. 36, no. 5, pp. 405–424, Sep. 1999.

WEI KUANG LAI received the B.S. degree in electrical engineering from National Taiwan University, Taipei, Taiwan, in 1984, and the Ph.D. degree in electrical engineering from Purdue University, West Lafayette, IN, in 1992. In 1992, he joined the Faculty of the Department of Computer Science and Engineering, National Sun Yat-sen University, Kaohsiung, Taiwan, where he is currently a Professor. His research interests include high-speed and wireless networks.

CHUNG-SHUO FAN received the M.S. degree in computer science and information engineering from the National Changhua University of Education, Changhua, Taiwan, in 2007, and the Ph.D. degree in computer science and engineering, National Sun Yat-sen University, Kaohsiung, Taiwan, in 2012. In 2016, he joined the Faculty of the Department of Information Management, Hsuan Chuang University, Hsinchu, Taiwan, where he is currently an Assistant Professor. His research interests include wireless sensor networks and vehicular ad hoc networks.